Available online at www.sciencedirect.com

ScienceDirect

International Journal of Solids and Structures 43 (2006) 6800–6816

INTERNATIONAL JOURNAL OF SOLIDS and STRUCTURES

www.elsevier.com/locate/ijsolstr

Free-edge stresses in antisymmetric angle-ply laminates in extension and torsion

Asghar Nosier *, Arash Bahrami

Department of Mechanical Engineering, Sharif University of Technology, P.O. Box 11365-9567, Azadi Avenue, Tehran, Iran

Received 23 July 2005; received in revised form 7 January 2006
Available online 6 March 2006

Communicated by David A. Hills

Abstract

The first-order shear deformation theory and the layerwise theory of laminated plates are employed to analyze the edge-effect problem of an antisymmetric angle-ply laminate subjected to arbitrary combinations of extensional and torsional loads. The first-order theory is used for predicting the unknown constant parameters appearing in the reduced displacement field of elasticity which, on the other hand, signify the global behavior of the laminate. A layerwise theory is then utilized to determine the local interlaminar stresses within the boundary-layer regions of laminates. In order to closely examine the behavioral characteristics of interlaminar stresses, various numerical examples are presented for different antisymmetric angle-ply laminates under an axial force and a torque.

Keywords: Antisymmetric angle-ply laminate; Interlaminar stresses; First-order shear deformation plate theory; Layerwise theory

1. Introduction

The applications of composite materials in structural members have extensively been grown in the recent decades. The edge-effect problem is a significant and fundamental issue concerned within the analysis of mechanical behavior characteristics of composite structures. It has already been recognized that the interlaminar edge stresses are one of the most important causes of the failure in composite laminates. Both experimental observations and approximate theoretical solutions have revealed existence of the boundary-layer regions in the vicinity of the edges where interlaminar stresses exhibit very large gradients. Numerous investigators have proposed various analytical and numerical methods to examine the transverse stress behavior near the edges of the laminate. A detailed description of the relevant literature can be found in the review article by Kant and Swaminathan (2000). The first complete analysis of interlaminar stresses is developed by Pipes and Pagano (1970). They formulated the edge-effect problem of a symmetric balanced laminate subjected to a uniform axial strain

* Corresponding author. Tel.: +98 21 6616 5543; fax: +98 21 66000021.
E-mail address: Nosier@Sharif.edu (A. Nosier).

0020-7683/$ - see front matter
doi:10.1016/j.ijsolstr.2006.02.006

as a quasi-three-dimensional problem and then used a finite difference technique to solve the governing equations of equilibrium. Rybicki (1971) proposed a three-dimensional finite element solution for the same problem. Based on the elasticity formulation presented by Pipes and Pagano (1970) and Pagano (1974) employed a higher-order displacement theory for estimation of transverse normal stress in axially loaded symmetric balanced laminates. An approximate elasticity solution is developed by Pipes and Pagano (1974) to study the nature of interlaminar stresses in symmetric angle-ply composite laminates due to a uniform axial strain. Hsu and Herakovich (1977a,b) obtained a zeroth-order perturbation solution for edge-effect problem of symmetric angle-ply laminates. An improved quasi-three-dimensional finite element method is proposed by Wang and Crossman (1977a,b) in order to determine the interlaminar stresses in symmetric balanced laminates under a uniform axial extension. Later, they used a similar approach to investigate through-the-thickness stresses due to thermal effects (1977). Spilker and Chou (1980) studied the edge-effect problem of symmetric balanced laminates by using a special hybrid-stress finite element method. A three-dimensional finite difference scheme is presented by Altus et al. (1980) for calculating interlaminar stresses in symmetric angle-ply laminates. Wang and Choi (1982a,b) employed an approach based on Lekhnitskii's complex variable potential to examine the free-edge stress singularities. In an attempt to efficient analysis of edge-effect problem of symmetric laminates, Kassapoglou and Lagace (1986) obtained a closed-form solution utilizing the force balanced method and the principle of minimum complementary energy. A similar technique to that of Kassapoglou and Lagace (1986) is presented by Webber and Morton (1993) to evaluate thermally induced interlaminar stresses. Based on the first-order shear deformation theory (FSDT) Rohwer et al. (2001) developed a method to compute interlaminar stresses in composite laminates subjected to thermal loading. Tahani and Nosier (2003, 2004) employed a layerwise theory (LWT) for accurate calculation of interlaminar stresses in a general cross-ply laminate subjected to extension, shearing, and hygrothermal loads. A comparative study between equivalent single-layer and layerwise theories for determination of transverse stress components under thermal loads is performed by Matsunaga (2004). Tian et al. (2004) attempted to present an efficient analysis for estimating interlaminar stresses in symmetric balanced laminates by means of a new three-dimensional hybrid-stress element. Recently, Nosier and Bahrami, in press, have developed an elasticity formulation for the edge-effect problem of an antisymmetric angle-ply laminate. Based on this formulation they used a layerwise theory (LWT) to investigate the interlaminar stress distributions in antisymmetric angle-ply laminates subjected to a constant axial strain.

From the literature survey it appears that very limited publications have been devoted to study the interlaminar stresses due to torsional loads (Whitney, 1994; Mitchel and Reddy, 2001). Furthermore, no paper has been published concerning the edge-effect problem in antisymmetric angle-ply laminates subjected to torsional loading. In the present paper, an efficient procedure for evaluating interlaminar stress components in antisymmetric angle-ply laminates under different types of extensional and torsional loads is presented. The main idea of the present method lies in the fact that in extension/torsion problem of an antisymmetric angle-ply laminate (Nosier and Bahrami, in press), each of the displacement components consists of two parts: a global part and a local part (also see Eq. (1) in the present paper). The unknown constants appearing in the global part of the displacement field may be determined accurately from an analysis based on FSDT. The unknown functions appearing in the local part, on the other hand, are determined from an analysis based on a layerwise theory in which full account is given to various three-dimensional and local effects.

2. Theoretical formulation

An antisymmetric angle-ply laminate (see e.g., Jones, 1998) subjected to a torque T_x and/or an axial force F_x at $x=-a$ and $x=a$ is considered here as shown in Fig. 1. The laminate is assumed to be long in the x-direction so that strains will be independent of x coordinate. In such a case, the most general form of the displacement field for the extension/torsion problem of antisymmetric angle-ply laminates is given by (see Nosier and Bahrami, in press)

$$\begin{aligned} u_1^{(k)}(x,y,z) &= B_2 x + u^{(k)}(y,z) \\ u_2^{(k)}(x,y,z) &= -B_1 xz + v^{(k)}(y,z) \\ u_3^{(k)}(x,y,z) &= B_1 xy + w^{(k)}(y,z) \end{aligned} \tag{1}$$

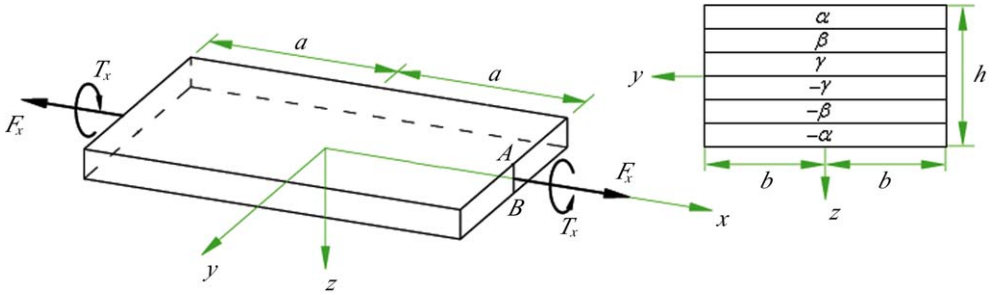

Fig. 1. Laminate geometry and coordinate system.

where $u_1^{(k)}(x,y,z)$, $u_2^{(k)}(x,y,z)$, and $u_3^{(k)}(x,y,z)$ denote the displacement components of a material point initially located at (x,y,z) in the kth lamina in the x-, y-, and z-directions, respectively, in the undeformed laminate. In Eq. (1) the unknown constants B_1 and B_2 and unknown functions $u^{(k)}(y,z)$, $v^{(k)}(y,z)$, and $w^{(k)}(y,z)$ correspond to global and local responses of the laminate, respectively (also see Nosier and Bahrami, in press). Therefore, FSDT is used here for determining B_1 and B_2. It is to be noted here that as it is shown by Nosier and Bahrami, in press, the constant B_2 represents the uniform axial strain in the x-direction. Also the quantity aB_1 is the angle of rotation of line AB about the x axis with $2a$ being the length of the laminate in the x-direction (see Fig. 1). In other words, within any theory if the quantities B_2 and B_1 are not specified to be known, then the axial force F_x and the torque T_x must be known. In contrast to the overall behavior of the laminate, analysis of the local responses such as stress field at the ply level may require the use of more complete theories. Thus, in the present study, a layerwise theory which possesses a full three-dimensional capability is employed to determine interlaminar stresses.

2.1. First-order shear deformation plate theory

In the first-order shear deformation plate theory (also known as Mindlin–Reissner plate theory) the displacement components are assumed to have the following form (see e.g., Reddy, 2003):

$$\begin{aligned} u_1(x,y,z) &= u(x,y) + z\psi_x(x,y) \\ u_2(x,y,z) &= v(x,y) + z\psi_y(x,y) \\ u_3(x,y,z) &= w(x,y) \end{aligned} \tag{2}$$

where u, v, and w are the middle plane displacements in the x-, y-, and z-directions, respectively. Also ψ_x and ψ_y denote rotations of the yz and xz planes in the laminate. Based on the displacement field in (1), it is concluded that, for the present problem, the general displacement field in (2) must take the following form:

$$\begin{aligned} u_1(x,y,z) &= B_2 x + u(y) + z\psi_x(y) \\ u_2(x,y,z) &= -B_1 xz + v(y) + z\psi_y(y) \\ u_3(x,y,z) &= B_1 xy + w(y) \end{aligned} \tag{3}$$

By starting from the displacement field in (3) and using the principle of minimum total potential energy (Fung and Tong, 2001), the equilibrium equations of the laminate in Fig. 1 are readily found to be

$$\delta u: \quad N'_{xy} = 0 \tag{4a}$$

$$\delta v: \quad N'_{y} = 0 \tag{4b}$$

$$\delta w: \quad Q'_{y} = 0 \tag{4c}$$

$$\delta \psi_x: \quad Q_x - M'_{xy} = 0 \tag{4d}$$

$$\delta \psi_y: \quad Q_y - M'_{y} = 0 \tag{4e}$$

$$\delta B_1: \quad T_x = \int_{-b}^{b} (yQ_x - M_{xy})\mathrm{d}y \tag{5a}$$

$$\delta B_2: \quad F_x = \int_{-b}^{b} N_x \mathrm{d}y \tag{5b}$$

in which a prime denotes ordinary differentiation with respect to the variable y.

Furthermore, the stress and moment resultants in (4) and (5) are defined as (see e.g., Reddy, 2003)

$$(N_x, N_y, M_y, M_{xy}, Q_x, Q_y) = \int_{-h/2}^{h/2} (\sigma_x, \sigma_y, z\sigma_y, z\sigma_{xy}, \sigma_{xz}, \sigma_{yz})\mathrm{d}z \tag{6}$$

Using the plane-stress Hooke law (Herakovich, 1998) together with the linear strain–displacement relations (Fung and Tong, 2001) the stress and moment resultants are expressed in terms of the displacement functions appearing in (3) which, on the other hand, may be presented as follows:

$$\begin{aligned}
&(N_x, N_y, M_{xy}) = (A_{11}, A_{12}, B_{16})B_2 + (A_{12}, A_{22}, B_{26})v' + (B_{16}, B_{26}, D_{66})(\psi_x' - B_1)\\
&(N_{xy}, M_y) = (A_{66}, B_{26})u' + (B_{26}, D_{22})\psi_y'\\
&Q_x = k_5^2 A_{55}(\psi_x + B_1 y) \quad \text{and} \quad Q_y = k_4^2 A_{44}(w' + \psi_y)
\end{aligned} \tag{7}$$

where A_{ij}, B_{ij}, and D_{ij} are laminate rigidities and k_i^2 $(i = 4, 5)$ are the shear correction factors introduced within FSDT in order to adjust the transverse shear rigidities (e.g., see Reddy, 2003). Upon substitution of (7) into Eqs. (4), the equilibrium equations are expressed in terms of the displacement components as follows:

$$\begin{aligned}
&\delta u: \quad A_{66}u'' + B_{26}\psi_y'' = 0\\
&\delta v: \quad A_{22}v'' + B_{26}\psi_x'' = 0\\
&\delta w: \quad k_4^2 A_{44}(w'' + \psi_y') = 0\\
&\delta \psi_x: \quad B_{26}v'' + D_{66}\psi_x'' - k_5^2 A_{55}\psi_x = k_5^2 A_{55} B_1 y\\
&\delta \psi_y: \quad B_{26}u'' + D_{22}\psi_y'' - k_4^2 A_{44}\psi_y - k_4^2 A_{44}w' = 0
\end{aligned} \tag{8}$$

Solving Eq. (8) subject to the traction-free boundary conditions at $y = -b$ and $y = b$ (i.e., $N_y = N_{xy} = Q_y = M_y = M_{xy} = 0$) results in $u(y) = w(y) = 0$. Also the functions $v(y)$, $\psi_x(y)$ and $\psi_y(y)$ are obtained in terms of the unknown constants B_1 and B_2. The former conclusion may alternatively be arrived at by making suitable arguments concerning the physical behavior of an antisymmetric angle-ply laminate under extensional and torsional loads (Nosier and Bahrami, in press). Next, upon substituting these results into the equilibrium equations in (5) the following relations are obtained:

$$\tfrac{1}{2}F_x = (2\overline{B}_{16}\bar{b})B_1 + (\overline{A}_{11}\tilde{b})B_2 \tag{9a}$$

$$\tfrac{1}{4}T_x = -(2\overline{D}_{66}\bar{b})B_1 + (\overline{B}_{16}\bar{b})B_2 \tag{9b}$$

where as it is mentioned earlier, F_x and the torque T_x are, respectively, an axial force and a torque applied at the ends of the laminate (i.e., at $x = a$ and $x = -a$). In addition, the constant parameters appearing in (9) are given in Appendix A. Solving Eqs. (9a) and (9b) result in

$$B_1 = \frac{1}{4}\frac{\overline{B}_{16}}{\overline{A}}F_x - \frac{1}{8}\frac{\overline{A}_{11}}{\overline{A}}\frac{\tilde{b}}{\bar{b}}T_x \tag{10a}$$

$$B_2 = \frac{1}{2}\frac{\overline{D}_{66}}{\overline{A}}F_x + \frac{1}{4}\frac{\overline{B}_{16}}{\overline{A}}T_x \tag{10b}$$

where

$$\overline{A} = \overline{A}_{11}\tilde{b}\overline{D}_{66} + \overline{B}_{16}^2\bar{b} \tag{11}$$

If the quantities B_2 and B_1 are specified, then relations (9) may be used to determine the axial force F_x and the torque T_x. On the other hand, if the axial force F_x and the torque T_x are specified, then relations (10) are used

to determine B_2 and B_1. For numerical purposes in the present study the following four loading cases will be considered:

$$\text{Loading case 1}: \quad T_x = T_0 \text{ and } F_x = 0 \tag{12a}$$

$$\text{Loading case 2}: \quad T_x = T_0 \text{ and } B_2 = 0 \tag{12b}$$

$$\text{Loading case 3}: \quad T_x = 0 \text{ and } F_x = F_0 \tag{12c}$$

$$\text{Loading case 4}: \quad B_1 = 0 \text{ and } F_x = F_0 \tag{12d}$$

where F_0 and T_0 indicate the prescribed values of axial force and torque, respectively. Clearly, loading cases 1 and 2 belong to torsion–extension problems and loading cases 3 and 4 correspond to extension–torsion problems. In other words, in loading cases 1 and 2 the specimen is subjected to a constant torque T_0 about the x-axis. In the first loading case the laminate is free from an axial force. In the second loading case, on the contrary, the laminate is constrained not to have any axial strain. On the other hand, in loading cases 3 and 4 the specimen is subjected to a tensile force F_0. In the former loading case the laminate is allowed to freely rotate about the x-axis while in the latter loading case it is restricted not to rotate about the x-axis. Next, relations (9) and (10) are used to determine the constants B_1 and B_2 appearing in (1) for the loading cases 1–4. The results are

$$\text{Loading case 1}: \quad B_1 = -\frac{1}{8}\frac{\overline{A}_{11}}{\overline{A}}\frac{\tilde{b}}{\bar{b}}T_0 \text{ and } B_2 = \frac{1}{4}\frac{\overline{B}_{16}}{\overline{A}}T_0 \tag{13a}$$

$$\text{Loading case 2}: \quad B_1 = -\frac{1}{8}\frac{1}{\overline{D}_{66}\bar{b}}T_0 \text{ and } B_2 = 0 \tag{13b}$$

$$\text{Loading case 3}: \quad B_1 = \frac{1}{4}\frac{\overline{B}_{16}}{\overline{A}}F_0 \text{ and } B_2 = \frac{1}{2}\frac{\overline{D}_{66}}{\overline{A}}F_0 \tag{13c}$$

$$\text{Loading case 4}: \quad B_1 = 0 \text{ and } B_2 = \frac{1}{2}\frac{1}{\overline{A}_{11}\tilde{b}}F_0 \tag{13d}$$

2.2. Layerwise laminated plate theory of Reddy

Here, in this section, the displacement-based layerwise theory of Reddy in which both transverse shear and normal effects are taken into account is employed to investigate the edge-effect problem of an antisymmetric angle-ply laminate. In general, the displacement field within LWT is assumed to be

$$\begin{aligned} u_1(x,y,z) &= u_k(x,y)\Phi_k(z) \\ u_2(x,y,z) &= v_k(x,y)\Phi_k(z) \quad k = 1,2,\ldots,N+1 \\ u_3(x,y,z) &= w_k(x,y)\Phi_k(z) \end{aligned} \tag{14}$$

with N being the total number of mathematical (or numerical) layers considered in a laminate. It is pointed out here that in (14) and in what follows a repeated index denotes summation from 1 to $N+1$. In Eq. (14) u_1, u_2, and u_3 represent the total displacement components, respectively, in the x-, y-, and z-directions of a material point located at (x,y,z) in the undeformed state. Also, the functions $u_k(x,y)$, $v_k(x,y)$, and $w_k(x,y)$ correspond to the values of the displacements u_1, u_2, and u_3 for points located on the kth surface (see Reddy, 2003). Moreover, $\Phi_k(z)$ are the global approximation functions of the thickness coordinate which are assumed here to be linear. These functions may be expressed, for convenience, in terms of the local Lagrangian interpolation functions as follows (Nosier et al., 1993):

$$\Phi_k(z) = \begin{cases} 0 & z \leqslant z_{k-1} \\ \Psi^2_{k-1}(z) & z_{k-1} \leqslant z \leqslant z_k \\ \Psi^1_k(z) & z_k \leqslant z \leqslant z_{k+1} \\ 0 & z \geqslant z_{k+1} \end{cases} \tag{15}$$

in which Ψ_k^j $(j = 1, 2)$ are defined as

$$\Psi_k^1(z) = \frac{1}{h_k}(z_{k+1} - z) \quad \text{and} \quad \Psi_k^2(z) = \frac{1}{h_k}(z - z_k) \tag{16}$$

Here h_k is the thickness of the kth mathematical layer. It is to be noted that in LWT each physical lamina can be divided into any desired finite number of mathematical layers with, of course, identical material properties and fiber orientation. The accuracy of LWT is clearly increased as each physical lamina is replaced by an increasing number of mathematical layers (see Nosier and Bahrami, in press; Nosier et al., 1993). Based on the displacement field in (1), it is evident that for the problem under consideration, the displacement field in (14) must take the following form:

$$\begin{aligned} u_1(x, y, z) &= B_2 x + U_k(y)\Phi_k(z) \\ u_2(x, y, z) &= -B_1 xz + V_k(y)\Phi_k(z) \quad k = 1, 2, \ldots, N+1 \\ u_3(x, y, z) &= B_1 xy + W_k(y)\Phi_k(z) \end{aligned} \tag{17}$$

Next, substitution of the displacement components in (17) into the three-dimensional strain–displacement relations of linear elasticity (Fung and Tong, 2001) leads to the following relations:

$$\begin{aligned} &\varepsilon_x = B_2, \quad \varepsilon_y = V_k'\Phi_k, \quad \varepsilon_z = W_k\Phi_k', \quad \gamma_{yz} = W_k'\Phi_k + V_k\Phi_k' \\ &\gamma_{xy} = U_k'\Phi_k - B_1 z, \quad \gamma_{xz} = U_k\Phi_k' + B_1 y \end{aligned} \tag{18}$$

Using the principle of minimum total potential energy (Fung and Tong, 2001), the equilibrium equations can readily be shown to be

$$\delta U_k: \quad Q_x^k - \frac{\mathrm{d}M_{xy}^k}{\mathrm{d}y} = 0 \tag{19a}$$

$$\delta V_k: \quad Q_y^k - \frac{\mathrm{d}M_y^k}{\mathrm{d}y} = 0 \tag{19b}$$

$$\delta W_k: \quad N_z^k - \frac{\mathrm{d}R_y^k}{\mathrm{d}y} = 0 \tag{19c}$$

$$\delta B_1: \quad T_x = \int_{-h/2}^{h/2}\int_{-b}^{b}(\sigma_{xz}y - \sigma_{xy}z)\mathrm{d}y\,\mathrm{d}z \tag{20a}$$

$$\delta B_2: \quad F_x = \int_{-h/2}^{h/2}\int_{-b}^{b}\sigma_x\,\mathrm{d}y\,\mathrm{d}z \tag{20b}$$

where the generalized stress resultants appearing in (19) are defined as

$$\begin{aligned} (M_y^k, M_{xy}^k, N_z^k) &= \int_{-h/2}^{h/2}(\sigma_y\Phi_k, \sigma_{xy}\Phi_k, \sigma_z\Phi_k')\mathrm{d}z \\ (Q_x^k, Q_y^k, R_y^k) &= \int_{-h/2}^{h/2}(\sigma_{xz}\Phi_k', \sigma_{yz}\Phi_k', \sigma_{yz}\Phi_k)\mathrm{d}z \end{aligned} \tag{21}$$

The stress–strain relations for the kth lamina of an orthotropic laminate, on the other hand, are given by (Herakovich, 1998)

$$\begin{Bmatrix} \sigma_x \\ \sigma_y \\ \sigma_z \\ \sigma_{yz} \\ \sigma_{xz} \\ \sigma_{xy} \end{Bmatrix}^{(k)} = \begin{bmatrix} \overline{C}_{11} & \overline{C}_{12} & \overline{C}_{13} & 0 & 0 & \overline{C}_{16} \\ \overline{C}_{12} & \overline{C}_{22} & \overline{C}_{23} & 0 & 0 & \overline{C}_{26} \\ \overline{C}_{13} & \overline{C}_{23} & \overline{C}_{33} & 0 & 0 & \overline{C}_{36} \\ 0 & 0 & 0 & \overline{C}_{44} & \overline{C}_{45} & 0 \\ 0 & 0 & 0 & \overline{C}_{45} & \overline{C}_{55} & 0 \\ \overline{C}_{16} & \overline{C}_{26} & \overline{C}_{36} & 0 & 0 & \overline{C}_{66} \end{bmatrix}^{(k)} = \begin{Bmatrix} \varepsilon_x \\ \varepsilon_y \\ \varepsilon_z \\ \gamma_{yz} \\ \gamma_{xz} \\ \gamma_{xy} \end{Bmatrix}^{(k)} \tag{22}$$

with $\overline{C}_{ij}^{(k)}$ being the ply off-axis stiffnesses. By substituting (18) into (22) and the subsequent results into (21) the stress resultants are found to be

$$\begin{aligned}(M_y^k, M_{xy}^k, N_z^k) &= (D_{26}^{kj}, D_{66}^{kj}, B_{36}^{jk})U_j' + (D_{22}^{kj}, D_{26}^{kj}, B_{23}^{jk})V_j' + (B_{23}^{kj}, B_{36}^{kj}, A_{33}^{kj})W_j \\ &\quad + (B_{12}^k, B_{16}^k, A_{13}^k)B_2 - (D_{26}^k, D_{66}^k, \overline{B}_{36}^k)B_1 \\ (Q_x^k, Q_y^k, R_y^k) &= (A_{55}^{kj}, A_{45}^{kj}, B_{45}^{kj})U_j + (A_{45}^{kj}, A_{44}^{kj}, B_{44}^{kj})V_j + (B_{45}^{jk}, B_{44}^{jk}, D_{44}^{kj})W_j' \\ &\quad + (A_{55}^k, A_{45}^k, B_{45}^k)B_1 y\end{aligned} \tag{23}$$

The rigidity terms appearing in (23) are, for convenience, given in Appendix B. Finally the displacement equilibrium equations, including $3(N+1)$ local equations and two global conditions, are obtained by substituting (23) into Eqs. (19) and (20), respectively

$$\delta U_k: \quad D_{66}^{kj}U_j'' - A_{55}^{kj}U_j + D_{26}^{kj}V_j'' - A_{45}^{kj}V_j + (B_{36}^{kj} - B_{45}^{jk})W_j' = B_1 A_{55}^k y \tag{24a}$$

$$\delta V_k: \quad D_{26}^{kj}U_j'' - A_{45}^{kj}U_j + D_{22}^{kj}V_j'' - A_{44}^{kj}V_j + (B_{23}^{kj} - B_{44}^{jk})W_j' = B_1 A_{45}^k y \tag{24b}$$

$$\delta W_k: \quad (B_{45}^{kj} - B_{36}^{jk})U_j' + (B_{44}^{kj} - B_{23}^{jk})V_j' + D_{44}^{kj}W_j'' - A_{33}^{kj}W_j = B_2 A_{13}^k - B_1(B_{45}^k + \overline{B}_{36}^k) \tag{24c}$$

and

$$\begin{aligned}T_x = \int_{-b}^{b} &[(A_{55}^j U_j + A_{45}^j V_j + B_{45}^j W_j')y - (D_{66}^j U_j' + D_{26}^j V_j' + \overline{B}_{36}^j W_j) \\ &+ B_1(A_{55}y^2 + D_{66}) - B_2 B_{16}]\mathrm{d}y\end{aligned} \tag{25a}$$

$$F_x = \int_{-b}^{b} (B_{16}^j U_j' + B_{12}^j V_j' + A_{13}^j W_j - B_1 B_{16} + B_2 A_{11})\mathrm{d}y \tag{25b}$$

where the stiffnesses A_{11}, A_{55}, B_{16}, and D_{66} are also defined in Appendix B. In order to analyze the free-edge effect problem of the laminate, the governing equilibrium equations within LWT (i.e., Eqs. (24) and (25)) must be solved subjected to the following traction-free boundary conditions at edges:

$$M_{xy}^k = M_y^k = R_y^k = 0 \quad \text{at } y = \pm b \tag{26}$$

3. Analytical solutions

The state space approach is utilized here to solve Eqs. (24a)–(24c) subjected to the boundary conditions in (26). For the sake of convenience the following state variables are introduced:

$$\begin{aligned}&\{\eta_1\} = \{U\}, \quad \{\xi_1\} = \{U'\} = \{\eta_1'\} \\ &\{\eta_2\} = \{V\}, \quad \{\xi_2\} = \{V'\} = \{\eta_2'\} \\ &\{\eta_3\} = \{W'\} = \{\xi_3'\}, \quad \{\xi_3\} = \{W\}\end{aligned} \tag{27}$$

where $\{\eta_1\}$ is a $(N+1)\times 1$ vector as follows:

$$\{\eta_1\}^{\mathrm{T}} = (U_1, U_2, U_3, \ldots, U_{N+1}) \tag{28}$$

The vectors $\{\eta_2\}$, $\{\eta_3\}$, $\{\xi_1\}$, $\{\xi_2\}$, and $\{\xi_3\}$ are also defined in a similar way. Substitution of (27) into (24) yields two systems of coupled first-order ordinary differential equations which may be presented as

$$\{\xi'\} = [A]\{\eta\} + \{P\}B_1 y \tag{29a}$$

and

$$\{\eta'\} = [B]\{\xi\} + \{F\}B_1 + \{\overline{F}\}B_2 \tag{29b}$$

in which

$$\{\eta\}^{\mathrm{T}} = (\{\eta_1\}^{\mathrm{T}}, \{\eta_2\}^{\mathrm{T}}, \{\eta_3\}^{\mathrm{T}}) \quad \text{and} \quad \{\xi\}^{\mathrm{T}} = (\{\xi_1\}^{\mathrm{T}}, \{\xi_2\}^{\mathrm{T}}, \{\xi_3\}^{\mathrm{T}}) \tag{30}$$

The coefficient matrices $[A]$ and $[B]$ and vectors $\{P\}$, $\{F\}$, and $\{\overline{F}\}$ appearing in Eqs. (29) are listed in Appendix C. As long as the boundary conditions at the edges parallel to x-axis (i.e., at $y = -b$ and $y = b$) are identical, the general solutions of Eqs. (29) may be written as (see Nosier and Bahrami, in press)

$$\begin{aligned}\{\xi\} &= [U][\cosh(\lambda y)]\{k_1\} - ([B]^{-1}\{F\} + [C]^{-1}\{P\})B_1 - [B]^{-1}\{\overline{F}\}B_2 \\ \{\eta\} &= [A]^{-1}[U][\Lambda][\sinh(\lambda y)]\{k_1\} - [A]^{-1}\{P\}B_1 y\end{aligned} \tag{31}$$

with matrices $[\cosh(\lambda y)]$ and $[\sinh(\lambda y)]$ being defined as

$$\begin{aligned}[\cosh(\lambda y)] &= \mathrm{diag}(\cosh(\lambda_1 y), \cosh(\lambda_2 y), \ldots, \cosh(\lambda_{3(N+1)} y)) \\ [\sinh(\lambda y)] &= \mathrm{diag}(\sinh(\lambda_1 y), \sinh(\lambda_2 y), \ldots, \sinh(\lambda_{3(N+1)} y))\end{aligned} \tag{32}$$

where λ_i^2 $(i = 1, 2, 3, \ldots, N+1)$ denote the eigenvalues of the matrix $[C] \equiv [A][B]$. Also $[U]$ is the modal matrix (i.e., matrix of eigenvectors) of the matrix $[C]$ and $[\Lambda]$ is a diagonal matrix which is defined as

$$[\Lambda] = \mathrm{diag}(\lambda_1, \lambda_2, \ldots, \lambda_{3(N+1)}) \tag{33}$$

In addition, the vector $\{k_1\}$ contains the $3(N+1)$ unknown integration constants. It should be noted that, in general, repeated zeros may exist among the eigenvalues of the matrix $[C]$. In order to avoid repeated eigenvalues, artificial terms $\alpha^{kj}U_j$, $\alpha^{kj}V_j$, and $\alpha^{kj}W_j$ are added to the right-hand sides of Eqs. (24a)–(24c), respectively, so that the eigenvalues of the matrix $[C]$ will all be distinct. Here, α^{kj} is, for convenience, defined to be

$$\alpha^{kj} = \alpha \int_{-h/2}^{h/2} \Phi_k \Phi_j \mathrm{d}z \tag{34}$$

where α is a relatively small number in comparison with rigidities A_{pq}^{kj} $(pq = 33, 44, 55)$. For more complete discussion on this subject the paper by Tahani and Nosier (2003) may be consulted.

It is reminded here that the unknown constants B_1 and B_2 appearing in (17) may be determined by two different approaches. In the first approach, B_1 and/or B_2 are assumed to be the same as those obtained from the first-order theory (FSDT). In the second approach, on the other hand, the layerwise theory may be used to compute these constants. This is readily accomplished with the help of global conditions in (25). Substitution of the solutions (31) and the conditions (12) into (25) and carrying out the integrations lead, in general, to a set of two algebraic equations. Solving these equations will yield B_1 and B_2 in terms of integration constants $\{k_1\}$. Next the vector $\{k_1\}$ is found by enforcing the boundary conditions in (26) only at one edge of the laminate, say, at $y = b$. Lastly, the coefficients B_1 and B_2 are found by merely substituting $\{k_1\}$ in the algebraic equations obtained from (25). The aforementioned procedure may be employed for determining B_1 and/or B_2 within LWT in all loading cases presented in (12). It is clear that in loading cases (12b) and (12d), in which one of the constants is specified at the outset, only one of the global equations in (25) are utilized to determine the remaining constant. It is to be noted that the significance of FSDT in accurate determination of B_1 and/or B_2 will become apparent when the numerical results for these constants are compared with those obtained within LWT.

4. Numerical results and discussions

In what follows, the distributions of the transverse stress components in antisymmetric angle-ply laminates are examined through various numerical examples. Layers with equal thicknesses (denoted by h_k) are assumed to have the following mechanical properties:

$$\begin{aligned}&E_1 = 132\ \mathrm{GPa}, \quad E_2 = E_3 = 10.8\ \mathrm{GPa}, \quad G_{12} = G_{13} = 5.65\ \mathrm{GPa} \\ &G_{23} = 3.38\ \mathrm{GPa}, \quad \nu_{12} = \nu_{13} = 0.24, \quad \nu_{23} = 0.59\end{aligned} \tag{35}$$

which belong to those of graphite/epoxy T300/5208 as given by Herakovich (1998). The value of 5/6 is used for the shear correction factors in FSDT (a number which is introduced by Reissner). In addition, each physical ply is modeled as being made up of, unless otherwise mentioned, 20 numerical layers within LWT (i.e., $p = 20$). In order to examine the accuracy of FSDT in predicting B_1 and B_2, these constants are also

determined according to LWT for several antisymmetric angle-ply laminates in all loading cases considered in (12). The results are presented for three values of width to thickness ratios $2b/h = 5$, 10, and 20 in Table 1 in which LC denotes the loading case. Furthermore, the thickness of each physical ply is assumed to be 0.5 mm (i.e., $h_k = 0.5$ mm) and the constants B_1 and B_2 are normalized, for the sake of convenience, so that (see Eqs. (13)) $\overline{B}_j = B_j/T_0$ $(j = 1, 2)$ for the loading cases 1 and 2 and $\overline{B}_j = B_j/F_0$ $(j = 1, 2)$ for the loading cases 3 and 4. It is observed that the deviation of FSDT solutions from LWT solutions is not large for thick laminates and is fairly small for thin laminates. Numerical study, however, indicates that the slight inaccuracy seen in FSDT in predicting these constants for thick laminates does not significantly influence the numerical values of stres-

Table 1
Numerical values of $\overline{B}_1$ and/or $\overline{B}_2$ for different width to thickness ratios according to FSDT and LWT

Laminate	LC[a]	Constants	Theory	$\frac{2b}{h} = 5$	$\frac{2b}{h} = 10$	$\frac{2b}{h} = 20$
[−80°/80°]	1	$\overline{B}_1$	FSDT	108.5584	49.0275	23.3826
			LWT	110.3445	49.3909	23.4645
		$\overline{B}_2$	FSDT	7.3727e−4	3.6864e−4	1.8432e−4
			LWT	7.5358e−4	3.7230e−4	1.8519e−4
	2	$\overline{B}_1$	FSDT	108.5289	49.0127	23.3752
			LWT	110.3165	49.3758	23.4570
	3	$\overline{B}_1$	FSDT	7.3727e−4	3.6863e−4	1.8432e−4
			LWT	7.5357e−4	3.7230e−4	1.8519e−4
		$\overline{B}_2$	FSDT	1.8430e−5	9.2153e−6	4.6077e−6
			LWT	1.8431e−5	9.2154e−6	4.6077e−6
	4	$\overline{B}_2$	FSDT	1.8425e−5	9.2126e−6	4.6062e−6
			LWT	1.8426e−5	9.2127e−6	4.6062e−6
[(10°/−10°)$_2$]	1	$\overline{B}_1$	FSDT	5.2336	2.4001	1.1527
			LWT	5.2420	2.4021	1.1532
		$\overline{B}_2$	FSDT	−3.4638e−4	−1.7319e−4	−8.6596e−5
			LWT	−3.5585e−4	−1.7541e−4	−8.7134e−5
	2	$\overline{B}_1$	FSDT	4.9582	2.2625	1.084
			LWT	4.9597	2.2616	1.084
	3	$\overline{B}_1$	FSDT	−3.4638e−4	−1.7319e−4	−8.6596e−5
			LWT	−3.5585e−4	−1.7541e−4	−8.7134e−5
		$\overline{B}_2$	FSDT	4.3570e−7	2.1785e−7	1.0892e−7
			LWT	4.4013e−7	2.1895e−7	1.0919e−7
	4	$\overline{B}_2$	FSDT	4.1277e−7	2.0535e−7	1.0242e−7
			LWT	4.1598e−7	2.0614e−7	1.0261e−7
[30°/90°/90°/−30°]	1	$\overline{B}_1$	FSDT	4.2040	1.9042	0.9144
			LWT	4.2399	1.9098	0.9154
		$\overline{B}_2$	FSDT	−2.2277e−3	−1.1138e−3	−5.5694e−4
			LWT	−2.2217e−3	−1.1123e−3	−5.5664e−4
	2	$\overline{B}_1$	FSDT	2.2661	0.9353	0.4299
			LWT	2.3348	0.9471	0.4323
	3	$\overline{B}_1$	FSDT	−2.2277e−3	−1.1139e−3	−5.5694e−4
			LWT	−2.2217e−3	−1.1123e−3	−5.5664e−4
		$\overline{B}_2$	FSDT	2.5611e−6	1.2805e−6	6.4026e−7
			LWT	2.5799e−6	1.2851e−6	6.4139e−7
	4	$\overline{B}_2$	FSDT	1.3806e−6	6.2896e−7	3.0104e−7
			LWT	1.4207e−6	6.3728e−7	3.0294e−7

[a] LC denotes the loading case.

ses (see also Nosier and Bahrami, in press). Hence, for calculating these constants, FSDT is certainly preferred over the computationally more involved layerwise theory. In the numerical examples that follow the interlaminar stresses are obtained by integrating the local equilibrium equations of elasticity. Also, the width to thickness ratio (i.e. $2b/h$) is assumed to be, unless otherwise mentioned, equal to 10. Furthermore, the stress components are normalized as

$$\bar{\sigma}_{ij} = \frac{\sigma_{ij}}{\sigma_0} \tag{36}$$

in which $\sigma_0 = F_0/bh$ for extension–torsion problems (i.e., loading cases 3 and 4) and $\sigma_0 = T_0/bh^2$ for the torsion–extension problems (i.e., loading cases 1 and 2).

4.1. Torsion–extension problems

Here in this section the laminates which are subjected to a torque T_0 (see Fig. 1) are considered and various numerical examples are presented for the loading cases 1 and 2 as defined in (12). The distributions of interlaminar stresses across the width of [60°/−30°/−60°/30°] laminate at 60°/−30° interface are presented in Fig. 2 for the loading case 1. It is seen that the interlaminar stresses exhibit high stress gradient near the free edge. Also, the maximum interfacial values of both σ_z and σ_{xz} at the 60°/−30° interface occurs at the free edge with the interlaminar shear stress σ_{xz} being larger than interlaminar normal stress σ_z. It is next noted that the transverse shear stress σ_{yz} becomes approximately (not exactly) equal to zero at the free edge. That is, the traction-free boundary condition at the free edge (i.e., $\sigma_{yz} = 0$ at $y = b$) is being satisfied with good approximation. Fig. 3 illustrates the interlaminar stress distributions along the middle plane of the [90°/45°/−45°/90°] laminate subjected to loading cases 1 and 2. It is observed that as far as σ_z is concerned the nature of the stress distributions is identical for both loading cases. On the contrary, the behavior of transverse shear stress σ_{xz} is

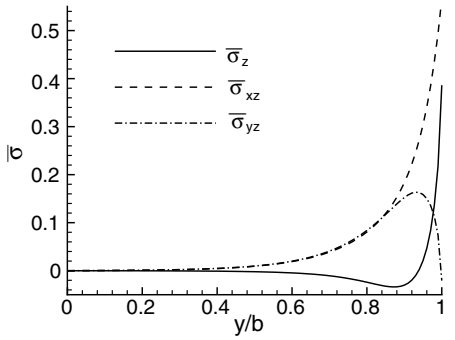

Fig. 2. Distributions of interlaminar stresses along the 60°/−30° interface of [60°/−30°/30°/−60°] laminate for loading case 1.

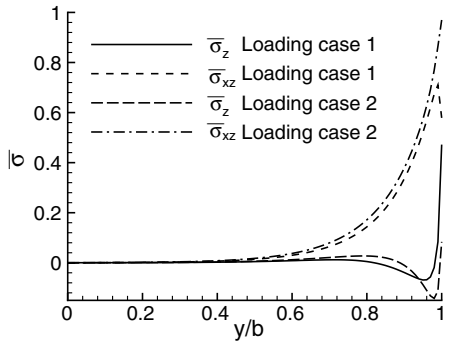

Fig. 3. Distributions of interlaminar stresses along the middle plane of [90°/45°/−45°/90°] laminate for loading cases 1 and 2.

different in the two loading cases. In loading case 1, σ_{xz} increases at first as the free edge is being approached and then suddenly decreases near the free edge (see Fig. 3). It is to be noted that the transverse shear stress σ_{yz} is found to be zero at the middle plane of antisymmetric angle-ply laminates subjected to all loading cases considered in the present paper (see Eqs. (12)). Through-the-thickness variation of transverse shear stress σ_{xz} is plotted in Fig. 4 in the vicinity of the free edge of the [90°/45°/0°/0°/−45°/90°] laminate under the loading case 1. It is observed that the distribution of transverse shear stress σ_{xz} is symmetric with respect to the middle plane. Also σ_{xz} attains its maximum value at the middle plane of the laminate. The distributions of the interlaminar normal stress through the thickness of [−15°/−45°/45°/15°] and [15°/−45°/45°/−15°] laminates at $y = b$ are compared with in Fig. 5 for the loading case 2. In both laminates the maximum negative stress occurs at the middle plane whereas the maximum positive stress occurs within the 45° and −45° layers. Also in the [−15°/−45°/45°/15°] laminate the maximum negative stress is quite larger than the maximum positive stress. This behavior is reversed in the [15°/−45°/45°/−15°] laminate. Fig. 6 displays the variations of the

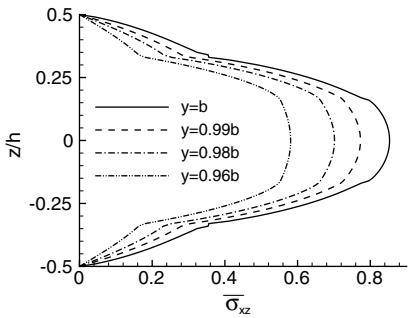

Fig. 4. Variations of interlaminar shear stress σ_{xz} through the thickness of [90°/45°/0°/0°/−45°/90°] laminate for loading case 1.

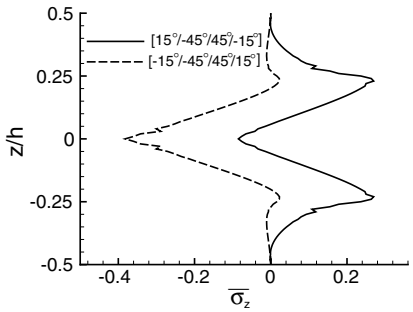

Fig. 5. Variations of interlaminar normal stress σ_z through the thickness of [−15°/−45°/45°/15°] and [15°/−45°/45°/−15°] laminates for loading case 2.

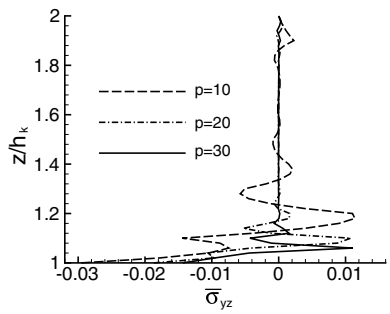

Fig. 6. Distribution of interlaminar shear stress σ_{yz} through the thickness of lowermost layer of $[(45°/-45°)_2]$ laminate for loading case 2.

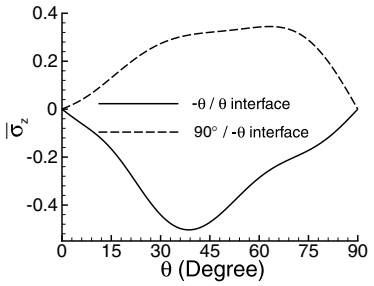

Fig. 7a. Interlaminar normal stress σ_z at the interface-edge junction of $[90°/-\theta/\theta/90°]$ laminate as a function of θ for loading case 1.

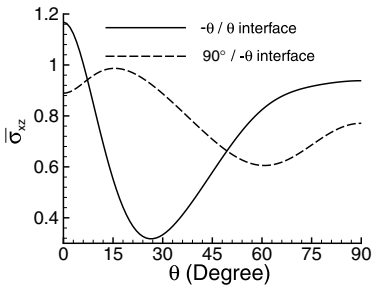

Fig. 7b. Interlaminar shear stress σ_{xz} at the interface-edge junction of $[90°/-\theta/\theta/90°]$ laminate as a function of θ for loading case 1.

interlaminar shear stress σ_{yz} at $y = b$ through the thickness of the lowermost layer in the $[(45°/-45°)_2]$ laminate for the loading case 2. It is seen that by increasing the number of numerical layers in each actual lamina the value of σ_{yz} approaches zero everywhere except at the interface-edge junction. Finally, variations of interlaminar stresses σ_z and σ_{xz} at various interface-edge junctions of the $[90°/-\theta/\theta/90°]$ laminate are depicted in Figs. 7a and 7b as a function of θ under the loading case 1. Fig. 7a indicates that the $90°/-\theta$ interface-edge junction exhibits a positive normal stress while the $-\theta/\theta$ interface-edge junction exhibits a negative normal stress for all values of θ. Also, it is found that σ_z attains its maximum value at the middle plane of $[90°/-39°/39°/90°]$ laminate (i.e., when $\theta = 39°$). Fig. 7b, on the other hand, reveals that the maximum of interlaminar shear stress σ_{xz} occurs at the middle plane of $[90°/0°/0°/90°]$ laminate. It is to be noted that because of the torsional load applied to the laminate, the transverse shear stress σ_{xz}, unlike the transverse normal stress σ_z, does not vanish in the $[90°/0°/0°/90°]$ and $[90°/90°/90°/90°]$ laminates. Moreover, closer numerical study indicates that the out-of-plane stress components σ_z and σ_{yz} are equal to zero everywhere in such laminates. This latter conclusion is seen to be valid for all symmetric cross-ply laminates subjected to the loading cases 1 and 2 (see Eqs. (12a) and (12b)).

4.2. Extension–torsion problems

The laminates which are subjected to an axial tensile force F_0 are considered here (see the loading cases 3 and 4 in Eqs. (12)). The effect of the laminate width to thickness ratio on the interlaminar stresses due to the loading case 3 is investigated in Figs. 8a and 8b in the $[0°/35°/-35°/0°]$ laminate. It is seen that the width of the boundary-layer regions always remains almost equal to the thickness of the laminate. That is, a thickness away from the edges of the laminate the interlaminar stresses approach zero. The out-of-plane stress distributions along the $-70°/90°$ interface of $[70°/-70°/90°/90°/70°/-70°]$ laminate are displayed in Fig. 9 for the loading case 4. It is observed that the maximum interfacial value of transverse normal stress σ_z is approximately 2.8 times greater than that of transverse shear stress σ_{xz}. In addition, it is observed that since instead of σ_{yz} the generalized stress resultants R_y^k are forced to vanish at the free edge in LWT, the numerical value of σ_{yz} may never become zero at the interface-edge junction (even by increasing the number of sublayers in each

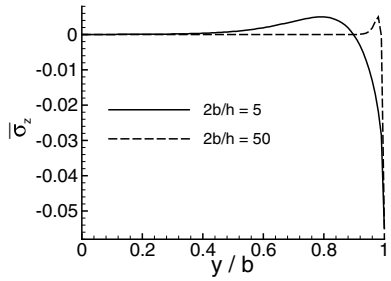

Fig. 8a. Interlaminar normal stress σ_z along the middle plane of [0°/35°/−35°/0°] laminate for various width to thickness ratios for loading case 3.

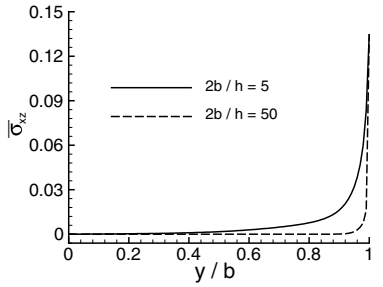

Fig. 8b. Interlaminar shear stress σ_{xz} along the middle plane of [0°/35°/−35°/0°] laminate for various width to thickness ratios for loading case 3.

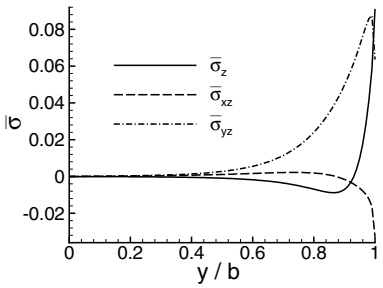

Fig. 9. Interlaminar stresses along the −70°/90° interface of [70°/−70°/90°/90°/70°/−70°] laminate for loading case 4.

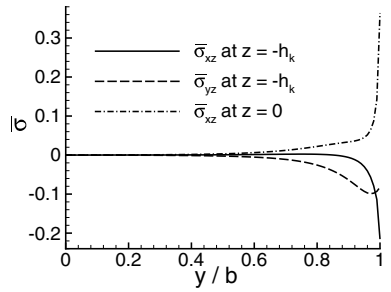

Fig. 10. Interlaminar shear stresses σ_{xz} and σ_{yz} at the interfaces of [−80°/45°/−45°/80°] laminate for loading case 3.

physical layer). The distributions of interlaminar shear stresses σ_{xz} and σ_{yz} along the interfaces of [−80°/45°/−45°/80°] laminate under the loading case 3 are illustrated in Fig. 10. It is seen that compared with the −80°/45° interface the boundary-layer width is larger for the 45°/−45° interface. It is again noticed that the

numerical value of σ_{yz} does not approach zero at the interface-edge junction. Fig. 11 illustrates the through-the-thickness distributions of the interlaminar stress components σ_z and σ_{xz} at the free-edge location in the [50°/−20°/0°/0°/20°/−50°] laminate for the loading case 4. It is seen that the interlaminar normal stress σ_z attains its maximum value at the middle surface of the laminate. The maximum of the interlaminar shear stress σ_{xz}, on the other hand, occurs near the 50°/−20° and 20°/−50° interfaces. The effect of fiber orientation θ on the free-edge interlaminar stresses σ_z and σ_{xz} is studied in Fig. 12 by plotting these stresses at the interface corner of $[\theta/-\theta]$ laminate due to the loading cases 3 and 4. It is observed that the transverse normal stress is notably larger for the loading case 3 whereas, on the other hand, the numerical values of interlaminar shear stress are not significantly affected by changing the loading case. The maximum value of σ_z occurs in the [42°/−42°] laminate in the loading case 3 (i.e., when the laminate is free to rotate). Also the maximum value of σ_{xz} occurs in the [39°/−39°] laminate in the loading case 4 (i.e., when the laminate is not allowed to rotate while being extended). Lastly, Fig. 13 shows the distributions of interlaminar stresses σ_z and σ_{xz} at the free edge as a function of fiber angle θ for two $\theta/-\theta$ interfaces of $[(\theta/-\theta)_3]$ laminate subjected to the loading case 4. It is observed that the location of the interface has a significant effect on the magnitude of the interlaminar stresses within the laminate. More specifically, for the interfaces chosen in Fig. 13, σ_z attains its maximum value, at

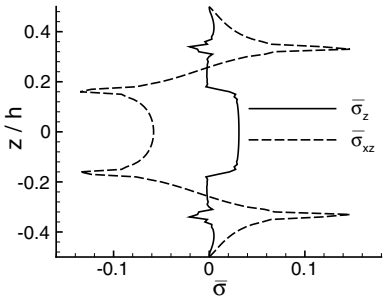

Fig. 11. Variations of interlaminar stresses σ_z and σ_{xz} through the thickness of [50°/−20°/0°/0°/20°/−50°] laminate for loading case 4.

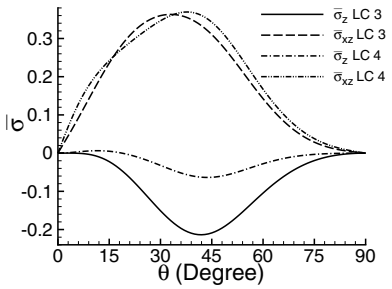

Fig. 12. Variations of interlaminar stresses σ_z and σ_{xz} at the interface-edge junction of $[\theta/-\theta]$ laminate versus θ for loading cases 3 and 4.

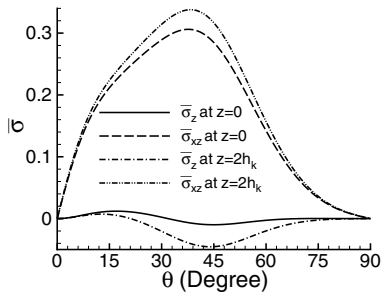

Fig. 13. Interlaminar stresses σ_z and σ_{xz} at the middle and bottom interface-edge junctions of $[(\theta/-\theta)_3]$ laminate as a function of θ for loading case 4.

$\theta = 45°$ in the bottom $\theta/-\theta$ interface whereas σ_{xz} becomes maximum at $\theta = 38°$ in the bottom $\theta/-\theta$ interface (i.e., at $z = 2h_k$).

5. Conclusions

In the present investigation, based on the elasticity formulation of the extension/torsion problem of long antisymmetric angle-ply laminates, analytical solutions are developed within both the first-order shear deformation plate theory (FSDT) and Reddy's layerwise theory (LWT) for the edge-effect problem of antisymmetric angle-ply laminates subjected to an axial force and/or a torque. The former theory is employed to determine the unknown constants B_1 and/or B_2 appearing in the appropriate displacement field of the problems and the latter one, on the other hand, is used to calculate interlaminar stresses within the laminate. Furthermore, the accuracy of FSDT in estimating these constants is assessed by comparing the FSDT results with those obtained within LWT. It is found that FSDT provides sufficiently accurate results so that actually no analysis based on LWT is required to determine B_1 and/or B_2. Finally, several numerical examples are presented for different antisymmetric angle-ply laminates under various extensional/torsional loading conditions.

Appendix A

The constant parameters appearing in (9) are defined as follows:

$$\overline{B}_{16} = \frac{A_{22}B_{16} - A_{12}B_{26}}{A_{22}}, \quad \overline{D}_{66} = \frac{A_{22}D_{66} - B_{26}^2}{A_{22}}, \quad \overline{A}_{11} = \frac{A_{11}A_{22} - A_{12}^2}{A_{22}}$$

and

$$\bar{b} = \frac{1}{\lambda}\tanh(\lambda b) - b, \quad \tilde{b} = b - \frac{\overline{B}_{16}^2}{\overline{A}_{11}\overline{D}_{66}}\frac{1}{\lambda}\tanh(\lambda b)$$

where

$$\lambda^2 = \frac{k_5^2 A_{55}}{\overline{D}_{66}}$$

Appendix B

The laminate rigidities, appearing in (23), are defined as

$$(A_{pq}^{kj}, B_{pq}^{kj}, D_{pq}^{kj}) = \sum_{i=1}^{N}\int_{z_i}^{z_{i+1}} \overline{C}_{pq}^{(i)}(\Phi_k'\Phi_j', \Phi_k\Phi_j', \Phi_k\Phi_j)\mathrm{d}z$$

$$(A_{pq}^{k}, B_{pq}^{k}, \overline{B}_{pq}^{k}, D_{pq}^{k}) = \sum_{i=1}^{N}\int_{z_i}^{z_{i+1}} \overline{C}_{pq}^{(i)}(\Phi_k', \Phi_k, \Phi_k'z, \Phi_k z)\mathrm{d}z$$

which may be presented in the following form (see also Nosier and Bahrami, in press; Nosier et al., 1993):

$$(A_{pq}^{kj}, B_{pq}^{kj}, D_{pq}^{kj}) = \begin{cases} \left(-\dfrac{\overline{C}_{pq}^{(k-1)}}{h_{k-1}}, -\dfrac{\overline{C}_{pq}^{(k-1)}}{2}, \dfrac{h_{k-1}\overline{C}_{pq}^{(k-1)}}{6}\right) & \text{if } j = k-1 \\ \left(\dfrac{\overline{C}_{pq}^{(k-1)}}{h_{k-1}} + \dfrac{\overline{C}_{pq}^{(k)}}{h_k}, \dfrac{\overline{C}_{pq}^{(k-1)}}{2} - \dfrac{\overline{C}_{pq}^{(k)}}{2}, \dfrac{h_{k-1}\overline{C}_{pq}^{(k-1)}}{3} + \dfrac{h_k\overline{C}_{pq}^{(k)}}{3}\right) & \text{if } j = k \\ \left(-\dfrac{\overline{C}_{pq}^{(k)}}{h_k}, \dfrac{\overline{C}_{pq}^{(k)}}{2}, \dfrac{h_k\overline{C}_{pq}^{(k)}}{6}\right) & \text{if } j = k+1 \\ (0,0,0) & \text{if } j < k-1 \text{ or } j > k+1 \end{cases}$$

and

$$(A^k_{pq}, B^k_{pq}, \overline{B}^k_{pq}, D^k_{pq}) = \begin{cases} \left(-\overline{C}^{(1)}_{pq}, \dfrac{h_1\overline{C}^{(1)}_{pq}}{2}, \overline{C}^{(1)}_{pq}\dfrac{z_1^2-z_2^2}{2h_1}, \dfrac{\overline{C}^{(1)}_{pq}}{h_1}\left[\dfrac{z_1^3-z_2^3}{3} - z_2\dfrac{z_1^2-z_2^2}{2}\right]\right) & \text{if } k=1 \\ \left(\overline{C}^{(k-1)}_{pq}, \dfrac{h_{k-1}\overline{C}^{(k-1)}_{pq}}{2}, \overline{C}^{(k-1)}_{pq}\dfrac{z_k^2-z_{k-1}^2}{2h_{k-1}}, \dfrac{\overline{C}^{(k-1)}_{pq}}{h_{k-1}}\left[\dfrac{z_k^3-z_{k-1}^3}{3} - z_{k-1}\dfrac{z_k^2-z_{k-1}^2}{2}\right]\right) & \text{if } k=N+1 \\ \left(\overline{C}^{(k-1)}_{pq} - \overline{C}^{(k)}_{pq}, \dfrac{h_{k-1}\overline{C}^{(k-1)}_{pq}}{2} + \dfrac{h_k\overline{C}^{(k)}_{pq}}{2}, \overline{C}^{(k-1)}_{pq}\dfrac{z_k^2-z_{k-1}^2}{2h_{k-1}} + \overline{C}^{(k)}_{pq}\dfrac{z_k^2-z_{k+1}^2}{2h_k},\right. & \\ \left.\dfrac{\overline{C}^{(k-1)}_{pq}}{h_{k-1}}\left[\dfrac{z_k^3-z_{k-1}^3}{3} - z_{k-1}\dfrac{z_k^2-z_{k-1}^2}{2}\right] + \dfrac{\overline{C}^{(k)}_{pq}}{h_k}\left[\dfrac{z_k^3-z_{k+1}^3}{3} - z_{k+1}\dfrac{z_k^2-z_{k+1}^2}{2}\right]\right) & \text{if } 1<k<N+1 \end{cases}$$

Also the rigidities A_{11}, A_{55}, B_{16}, and D_{66} appearing in (25) are defined as follows:

$$(A_{11}, A_{55}) = \int_{-h/2}^{h/2} (\overline{C}_{11}, \overline{C}_{55})\mathrm{d}z, \quad B_{16} = \int_{-h/2}^{h/2} \overline{C}_{16} z\,\mathrm{d}z, \quad \text{and} \quad D_{66} = \int_{-h/2}^{h/2} \overline{C}_{66} z^2 \mathrm{d}z$$

where $\overline{C}_{pq}$'s are the transformed (off-axis) stiffnesses.

Appendix C

The coefficient matrices $[A]$ and $[B]$ and vectors $\{P\}$, $\{F\}$ and $\{\overline{F}\}$ appearing in (29) are given as follows:

$$[A] = \begin{bmatrix} [a_1] & [a_2] & [a_3] \\ [b_1] & [b_2] & [b_3] \\ [0] & [0] & [I] \end{bmatrix}, \qquad [B] = \begin{bmatrix} [I] & [0] & [0] \\ [0] & [I] & [0] \\ [c_1] & [c_2] & [c_3] \end{bmatrix}$$

$$\{F\} = \begin{Bmatrix} \{0\} \\ \{0\} \\ \{c_4\} \end{Bmatrix}, \quad \{\overline{F}\} = \begin{Bmatrix} \{0\} \\ \{0\} \\ \{c_5\} \end{Bmatrix}, \quad \{P\} = \begin{Bmatrix} \{a_4\} \\ \{b_4\} \\ \{0\} \end{Bmatrix}$$

in which [0] and $[I]$ are $(N+1)\times(N+1)$ square zero and identity matrices, respectively, and $\{0\}$ is a zero vector with $(N+1)$ rows. Furthermore

$$[a_1] = [\bar{a}_1]^{-1}[\bar{a}_2], \quad [a_2] = [\bar{a}_1]^{-1}[\bar{a}_3], \quad [a_3] = [\bar{a}_1]^{-1}[\bar{a}_4], \quad \{a_4\} = [\bar{a}_1]^{-1}\{\bar{a}_5\}$$
$$[b_1] = [D_{22}]^{-1}([A_{45}] - [D_{26}][a_1]), \quad [b_2] = [D_{22}]^{-1}([A_{44}] + [\alpha] - [D_{26}][a_2])$$
$$[b_3] = [D_{22}]^{-1}([B_{44}]^{\mathrm{T}} - [B_{23}] - [D_{26}][a_3]), \quad \{b_4\} = [D_{22}]^{-1}(\{A_{45}\} - [D_{26}]\{a_4\})$$
$$[c_1] = [D_{44}]^{-1}([B_{36}]^{\mathrm{T}} - [B_{45}]), \quad [c_2] = [D_{44}]^{-1}([B_{23}]^{\mathrm{T}} - [B_{44}])$$
$$[c_3] = [D_{44}]^{-1}([A_{33}] + [\alpha]), \quad \{c_4\} = -[D_{44}]^{-1}(\{B_{45}\} + \{\overline{B}_{36}\}), \quad \{c_5\} = [D_{44}]^{-1}\{A_{13}\}$$

where

$$[\bar{a}_1] = [D_{66}] - [D_{26}][D_{22}]^{-1}[D_{26}], \quad [\bar{a}_2] = [A_{55}] + [\alpha] - [D_{26}][D_{22}]^{-1}[A_{45}]$$
$$[\bar{a}_3] = [A_{45}] - [D_{26}][D_{22}]^{-1}([A_{44}] + [\alpha]), \quad [\bar{a}_4] = [B_{45}]^{\mathrm{T}} - [B_{36}] + [D_{26}][D_{22}]^{-1}([B_{23}] - [B_{44}]^{\mathrm{T}})$$
$$\{\bar{a}_5\} = \{A_{55}\} - [D_{26}][D_{22}]^{-1}\{A_{45}\}$$

References

Altus, E., Rotem, A., Shmueli, M., 1980. Free edge effect in angle-ply laminate-a new three dimensional finite difference solution. Journal of Composite Materials 14, 21–30.

Fung, Y.C., Tong, P., 2001. Classical and Computational Solid Mechanics. World Scientific, New Jersey.
Herakovich, C.T., 1998. Mechanics of Fibrous Composites. John Wiley & Sons, New York.
Hsu, P.W., Herakovich, C.T., 1977a. A perturbation solution for interlaminar stresses in bidirectional laminates. In: Composite Materials Testing and Design, 4th Conference, ASTM STP 617, pp. 296–316.
Hsu, P.W., Herakovich, C.T., 1977b. Edge effects in angle-ply composite laminates. Journal of Composite Materials 11, 422–428.
Jones, R.M., 1998. Mechanics of Composite Materials. Taylor & Francis, London.
Kant, T., Swaminathan, K., 2000. Estimation of transverse/interlaminar stresses in laminated composites—a selective review and survey of current developments. Composite Structures 49, 65–75.
Kassapoglou, C., Lagace, P.A., 1986. An efficient method for the calculation of interlaminar stresses in composite materials. Journal of Applied Mechanics 53, 744–750.
Matsunaga, H., 2004. A comparison between 2-D single-layer and 3-D layerwise theories for computing interlaminar stresses of laminated composite and sandwich plates subjected to thermal loadings. Composite Structures 64, 161–177.
Mitchel, J.A., Reddy, J.N., 2001. Study of interlaminar stresses in composite laminates subjected to torsional loading. AIAA Journal 39 (7), 1374–1382.
Nosier, A., Bahrami, A., in press. Interlaminar stresses in antisymmetric angle-ply laminates. Composite Structures.
Nosier, A., Kapania, R.K., Reddy, J.N., 1993. Free vibration analysis of laminated plates using a layerwise theory. AIAA Journal 13 (12), 2335–2346.
Pagano, N.J., 1974. On the calculation of interlaminar normal stress in composite laminate. Journal of Composite Materials 8, 65–81.
Pipes, R.B., Pagano, N.J., 1970. Interlaminar stresses in composite laminates under uniform axial extension. Journal of Composite Materials 4, 538–548.
Pipes, R.B., Pagano, N.J., 1974. Interlaminar stresses in composite laminates-an approximate elasticity solution. Journal of Applied Mechanics 41, 668–672.
Reddy, J.N., 2003. Mechanics of Laminated Composite Plates and Shells: Theory and Analysis. CRC Press, New York.
Rohwer, K., Rolfes, R., Sparr, H., 2001. Higher-order theories for thermal stresses in layered plates. International Journal of Solids and Structures 38, 3673–3687.
Rybicki, E.F., 1971. Approximate three-dimensional solutions for symmetric laminates under inplane loading. Journal of Composite Materials 5, 354–360.
Spilker, R.L, Chou, S.C., 1980. Edge effects in symmetric composite laminates: importance of satisfying the traction-free-edge condition. Journal of Composite Materials 14, 2–20.
Tahani, M., Nosier, A., 2003. Free edge stress analysis of general cross-ply composite laminates under extension and thermal loading. Composite Structures 60, 91–103.
Tahani, M., Nosier, A., 2004. Accurate determination of interlaminar stresses in general cross-ply laminates. Mechanics of Advanced Materials and Structures 11 (1), 67–92.
Tian, Z., Zhao, F., Yang, Q., 2004. Straight free-edge effects in laminated composites. Finite Elements in Analysis and Design 41, 1–14.
Wang, A.S.D., Crossman, F.W., 1977a. Some new results on edge effect in symmetric composite laminates. Journal of Composite Materials 11, 92–106.
Wang, A.S.D., Crossman, F.W., 1977b. Edge effects on thermally induced stresses in composite laminates. Journal of Composite Materials 11, 300–312.
Wang, S.S., Choi, I., 1982a. Boundary-layer effects in composite laminates. Part I: Free-edge stress singularities. Journal of Applied Mechanics 49, 541–548.
Wang, S.S., Choi, I., 1982b. Boundary layer effects in composite laminates. Part II: Free-edge stress solutions and basic characteristic. Journal of Applied Mechanics 49, 549–560.
Webber, J.P.H., Morton, S.K., 1993. An analytical solution for the thermal stresses at the free edges of laminated plates. Composite Science and Technology 46, 175–185.
Whitney, J.M., 1994. Analysis of interlaminar stresses in the torsion of symmetric laminates. AIAA Journal 32 (3), 662–665.